ELSEVIER

Journal of Magnetism and Magnetic Materials 138 (1994) 307–313

Journal of magnetism and magnetic materials

Crystal and magnetic structures of U_2Ni_2Sn investigated by neutron diffraction and ^{119}Sn Mössbauer spectroscopy

F. Bourée [a,*], B. Chevalier [b], L. Fournès [b], F. Mirambet [b], T. Roisnel [a], V.H. Tran [a,c], Z. Zołnierek [c]

[a] *Laboratoire Léon Brillouin, CEA-CNRS, CE-Saclay, 91191 Gif-Sur-Yvette Cedex, France*

[b] *Laboratoire de Chimie du Solide du CNRS, 351 Cours de la Libération, 33405 Talence Cedex, France*

[c] *W. Trzebiatowski Institute of Low Temperature and Structure Research, Polish Academy of Sciences, 50-950 Wroclaw, Poland*

Received 21 February 1994; in revised form 8 June 1994

Abstract

The U_2Ni_2Sn stannide has been studied by means of neutron powder diffraction and Mössbauer spectroscopy. This compound crystallizes in the tetragonal P4/mbm space group in an ordered version of the U_3Si_2-type structure and orders antiferromagnetically below $T_N = 25(1)$ K. At $T = 1.5$ K the magnetic structure is collinear with uranium magnetic moment ($1.05(5)\mu_B$) perpendicular to the tetragonal c-axis. ^{119}Sn Mössbauer spectroscopy at 4.2 K shows that tin atoms see a zero hyperfine field, in agreement with the proposed antiferromagnetic order.

1. Introduction

During the last few years the magnetic properties of several families of ternary uranium compounds, for instance UTX, UT_2X and UT_2X_2 (T is a transition element, X a metalloid) have attracted a great deal of interest [1]. The reason is simple: the existence of a family of uranium compounds provides an excellent opportunity to make a comparative study of their electronic and magnetic properties and to look at the development of the 5f-ligand hybridization effects within the investigated series. Recently Mirambet et al. [2] have discovered a new family of uranium stannides: U_2T_2Sn. These compounds crystallize in the P4/mbm tetragonal space group, in an ordered version of the U_3Si_2-type structure [3]. This discovery stimulated many workers to study the magnetic properties of the U_2T_2X series: from electrical resistivity, specific heat and magnetic measurements [4–8], it was shown that most of the U_2T_2Sn phases exhibit antiferromagnetic order at low temperatures. In this paper we focus on the magnetic structure of U_2Ni_2Sn, studied by neutron powder diffraction and ^{119}Sn Mössbauer spectroscopy. Susceptibility measurements indicate that U_2Ni_2Sn is antiferromagnetic below $T_N = 29.7$ K [4] or 25(1) K [7].

2. Experimental

The experiments were performed on two different U_2Ni_2Sn samples. Sample 1 was prepared by melting stoichiometric amounts of the constituent elements in an induction levitation furnace under a purified argon atmosphere. It was then vacuum annealed at 800°C for two weeks. Sample 2 was synthesized by arc melting

* Corresponding author.

SSDI 0304-8853(94)00430-Y

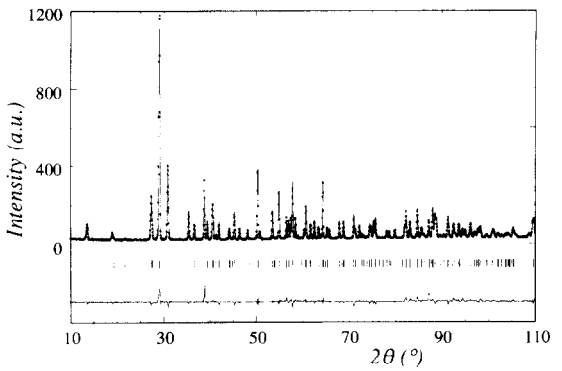

Fig. 1. Observed ($\lambda = 1.2259$ Å) and calculated neutron diffraction patterns at $T = 300$ K for U_2Ni_2Sn (full circles: observed, continuous lines: calculated and difference profile).

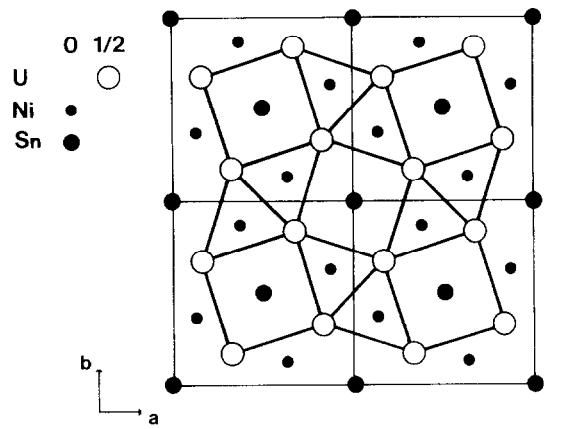

Fig. 2. Projection of the U_2Ni_2Sn crystal structure on the (a,b) plane.

the constituent elements on a water-cooled copper hearth under argon gas and was not annealed. Microprobe analysis of both samples indicates that the obtained stannides are single phase and that their composition corresponds to the nominal concentration.

Neutron powder diffraction measurements were carried out at the Orphée reactor (CE-Saclay, France), on the 2-axis diffractometer 3T2 (high-resolution powder diffractometer, $\lambda = 1.2259$ Å) at 300 K and G4.1 ($\lambda = 2.426$ Å; 800-cells position-sensitive detector) at $T = 36$ and 1.5 K. The data were analyzed with the Rietveld-type program FULLPROF [9], using neutron scattering lengths from [10] and U^{3+} magnetic form factor from [11].

^{119}Sn Mössbauer measurements were performed using a $CaSnO_3$ source and a conventional constant acceleration spectrometer. The isomer shifts (IS) were quoted relative to $CaSnO_3$.

3. Results

3.1. Crystal structure

The neutron powder diffraction pattern at room temperature (Fig. 1) shows that U_2Ni_2Sn is isostructural with U_2T_2Sn (T = Fe or Rh) [2]. These compounds crystallize in the ordered version of the U_3Si_2-type structure [3], in the P4/mbm space group:

U	(4h)	x	$\frac{1}{2}+x$	$\frac{1}{2}$	[U]
Ni	(4g)	x	$\frac{1}{2}+x$	0	[Si]
Sn	(2a)	0	0	0	[U]

This structure has already been described in detail by Mirambet et al. [2]; it can be considered as a stacking of atomic planes perpendicular to the c-axis, with the sequence: (Ni,Sn)–U–(Ni,Sn)–U (Fig. 2).

The crystallographic parameters (a, c, x_U, x_{Ni}, Debye–Waller thermal factors), determined from Rietveld profile refinement of 3T2 data on U_2Ni_2Sn, are listed in Table 1.

In the U_2Ni_2Sn crystal structure, the 'big' U and Sn atoms are located on the (4h) and (2a) uranium sites

Table 1
U_2Ni_2Sn, $T = 300$ K: lattice and atomic positions parameters, isotropic temperature factors, obtained from neutron powder diffraction (Fig. 1; $R_p = 6.55\%$, $R_{wp} = 8.45\%$, $R_B = 8.75\%$)

Space group: P 4/mbm		$a = 7.2690(2)$ Å		$c = 3.6929(1)$ Å	
Atom	Site	x	y	z	B_{iso} (Å^2)
U	(4h)	0.1739(2)	0.6739(2)	0.5	0.65(3)
Ni	(4g)	0.3750(2)	0.8750(2)	0	0.84(2)
Sn	(2a)	0	0	0	0.70(4)

Table 2
Atomic distances up to 4 Å in the U_2Ni_2Sn compound ($T=300$ K)

U–4U = 3.799(1) Å	Ni–4U = 2.873(1) Å	Sn–8U = 3.260(1) Å
U–2U = 3.693(1) Å	Ni–2U = 2.772(1) Å	
U–1U = 3.575(1) Å		
U–4Sn = 3.260(1) Å	Ni–2Sn = 2.873(1) Å	Sn–2Sn = 3.693(1) Å
U–4Ni = 2.873(1) Å	Ni–2Ni = 3.693(1) Å	Sn–4Ni = 2.873(1) Å
U–2Ni = 2.772(1) Å	Ni–1Ni = 2.570(1) Å	

of U_3Si_2, whereas the 'small' Ni atoms are assigned to the (4g) silicium site, leading to relatively large d_{U-U} and d_{Sn-Sn} distances and a shorter d_{Ni-Ni} distance (Table 2). It must be noted that all the d_{U-U} values in U_2Ni_2Sn are greater than the Hill critical limit of 3.50 Å [12], below which an overlap between the 5f orbitals can occur and lead to a non-magnetic ground state for uranium.

3.2. Magnetic structure

G4.1 ($\lambda=2.426$ Å) neutron powder diffraction patterns of U_2Ni_2Sn at low temperature ($T=36$ and 1.5 K) are shown on Fig. 3.

At 36 K, this pattern exhibits only nuclear contributions, in good agreement with the room-temperature crystal structure. The following lattice parameters have been obtained: $a=7.214(3)$ Å and $c=3.707(2)$ Å.

At $T=1.5$ K (Fig. 3b), some superstructure Bragg peaks appear, that cannot be indexed in the nuclear unit cell, but in a $(a\times a\times 2c)$ magnetic cell: they are then labelled as (101), (111) and (211). These superstructure peaks can also be referenced as $100^{\pm}$, $110^{\pm}$ and $210^{\pm}$, with a wavevector $\boldsymbol{k}=(0, 0, 1/2)$.

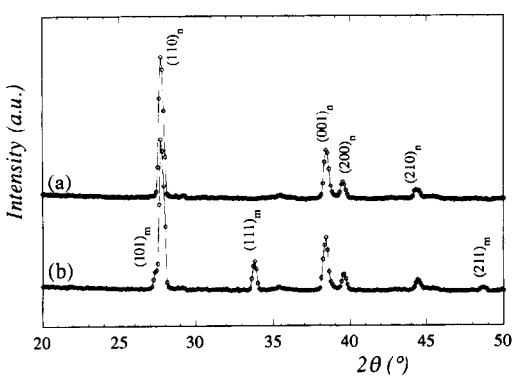

Fig. 3. Neutron diffraction patterns ($\lambda=2.426$ Å) of U_2Ni_2Sn at $T=36$ K (a) and 1.5 K (b).

Symmetry analysis (magnetic group theory) can provide relations between the magnetic moments of the different uranium atoms in the crystalline unit cell, namely:

$$U_1 \quad (x \quad \tfrac{1}{2}+x \quad \tfrac{1}{2}),$$

$$U_2 \quad (-x \quad \tfrac{1}{2}-x \quad \tfrac{1}{2}),$$

$$U_3 \quad (\tfrac{1}{2}+x \quad -x \quad \tfrac{1}{2}),$$

and $$U_4 \quad (\tfrac{1}{2}-x \quad x \quad \tfrac{1}{2}).$$

The wavevector $\boldsymbol{k}=\frac{1}{2}\boldsymbol{c}^*$ is invariant under all the rotational parts of the elements of the (space) group P4/mbm: these elements (Γ_k group) are listed in Table 3, together with the associated irreducible representations Γ_i [13]. The representation Γ, which describes the transformation properties of the $4\times 3=12$ components of the U_i magnetic moments ($i=1,\ldots,4$) under the elements of the space group G is a reducible representation of G. From the values of its characters:

$$\chi(h_1)=12, \quad \chi(h_{28})=4,$$

$$\chi(h_{13})=\chi(h_{16})=2, \quad \chi(h_{37})=\chi(h_{40})=-2$$

and

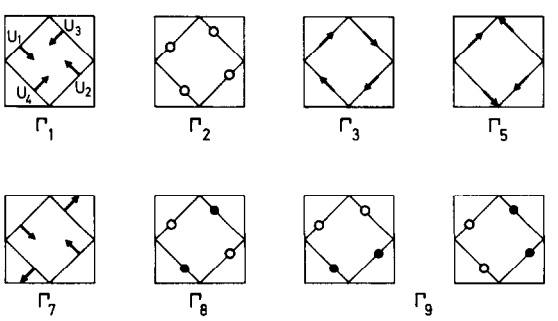

Fig. 4. Symmetry analysis of the 2:2:1 magnetic structures (wave vector $\boldsymbol{k}=\frac{1}{2}\boldsymbol{c}^*$): magnetic moments of the U atoms at $z=\frac{1}{4}$.

Table 3
Irreducible representations of the G_k group: $\{h_1=(x\,y\,z)$, $h_{14}=(-y\,x\,z)$, $h_4=(-x\,-y\,z)$, $h_{15}=(y\,-x\,z)$, $h_2=(x\,-y\,-z)$, $h_{13}=(-y\,-x\,-z)$, $h_3=(-x\,y\,-z)$, $h_{16}=(y\,x\,-z)$ and $h_{n+24}=h_n*(-x\,-y\,-z)\}$ for $\boldsymbol{k}=0$ or $\boldsymbol{k}=\frac{1}{2}\boldsymbol{c}^*$

	h_1	h_{14}	h_4	h_{15}	h_2	h_{13}	h_3	h_{16}	h_{25}	h_{38}	h_{28}	h_{39}	h_{26}	h_{37}	h_{27}	h_{40}
Γ_1	1	1	1	1	1	1	1	1	1	1	1	1	1	1	1	1
Γ_2	1	1	1	1	1	1	1	1	−1	−1	−1	−1	−1	−1	−1	−1
Γ_3	1	1	1	1	−1	−1	−1	−1	1	1	1	1	−1	−1	−1	−1
Γ_4	1	1	1	1	−1	−1	−1	−1	−1	−1	−1	−1	1	1	1	1
Γ_5	1	−1	1	−1	1	−1	1	−1	1	−1	1	−1	1	−1	1	−1
Γ_6	1	−1	1	−1	1	−1	1	−1	−1	1	−1	1	−1	1	−1	1
Γ_7	1	−1	1	−1	−1	1	−1	1	1	−1	1	−1	−1	1	−1	1
Γ_8	1	−1	1	−1	−1	1	−1	1	−1	1	−1	1	1	−1	1	−1
Γ_9	1 0	i 0	−1 0	−i 0	0 1	0 −i	0 −1	0 i	1 0	i 0	−1 0	−i 0	0 1	0 −i	0 −1	0 i
	0 1	0 −i	0 −1	0 i	1 0	i 0	−1 0	−i 0	0 1	0 −i	0 −1	0 i	1 0	i 0	−1 0	−i 0
Γ_{10}	1 0	i 0	−1 0	−i 0	0 1	0 −i	0 −1	0 i	−1 0	−i 0	1 0	i 0	0 −1	0 i	0 1	0 −i
	0 1	0 −i	0 −1	0 i	1 0	i 0	−1 0	−i 0	0 −1	0 i	0 1	0 −i	−1 0	−i 0	1 0	i 0

$$\chi(h_{14})=\chi(h_4)=\chi(h_{15})=\chi(h_2)$$
$$=\chi(h_3)=\chi(h_{25})=\chi(h_{38})$$
$$=\chi(h_{39})=\chi(h_{26})=\chi(h_{27})=0,$$

we obtain:

$$\Gamma=\Gamma_1+\Gamma_2+\Gamma_3+\Gamma_5+\Gamma_7+\Gamma_8+\Gamma_9+2\times\Gamma_{10}.$$

The basis vectors of each of these representations are obtained by using the projection operator method and are reported in Fig. 4:

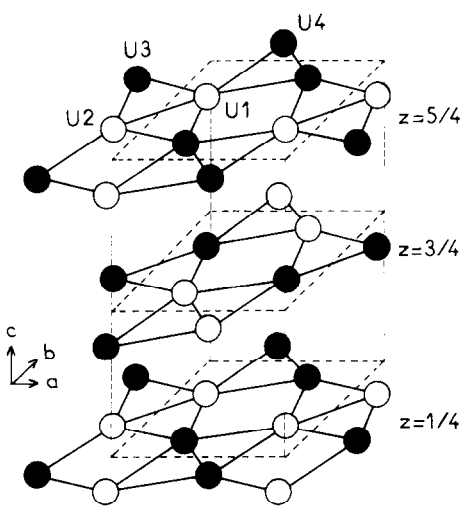

Fig. 5. Magnetic structure of U_2Ni_2Sn at 1.5 K. Only the U atoms are represented in this figure: their magnetic moments are located in the $(\boldsymbol{a},\boldsymbol{b})$ plane; full and open circles indicate opposite magnetic moments.

Γ_1: $(M_{1x}-M_{1y})-(M_{2x}-M_{2y})$
$-(M_{3x}+M_{3y})+(M_{4x}+M_{4y})$

Γ_2: $(M_{1z}+M_{2z}+M_{3z}+M_{4z})$

Γ_3: $(M_{1x}+M_{1y})-(M_{2x}+M_{2y})$
$+(M_{3x}-M_{3y})-(M_{4x}-M_{4y})$

Γ_5: $(M_{1x}+M_{1y})-(M_{2x}+M_{2y})$
$-(M_{3x}-M_{3y})+(M_{4x}-M_{4y})$

Γ_7: $(M_{1x}-M_{1y})-(M_{2x}-M_{2y})$
$+(M_{3x}+M_{3y})-(M_{4x}+M_{4y})$

Γ_8: $(M_{1z}+M_{2z}-M_{3z}-M_{4z})$

Γ_9: $(M_{1z}-M_{2z})+(M_{3z}-M_{4z})$
and $(M_{1z}-M_{2z})-(M_{3z}-M_{4z})$

Γ_{10}: $(M_{1x}+M_{2x})\pm i(M_{3y}+M_{4y})$
and $(M_{1y}+M_{2y})\pm i(M_{3x}+M_{4x})$

In the last case (Γ_{10}) every solution in the $(\boldsymbol{a},\boldsymbol{b})$ plane is possible under the condition $\boldsymbol{M}_1=\boldsymbol{M}_2$ and $\boldsymbol{M}_3=\boldsymbol{M}_4$.

The best fit ($R_B=8.95\%$) between observed and calculated magnetic Bragg peaks is obtained with Γ_{10}. The U_2Ni_2Sn magnetic structure is described below (coordinates of the U atoms in the magnetic unit cell $(a\times a\times 2c)$) and shown in Fig. 5:

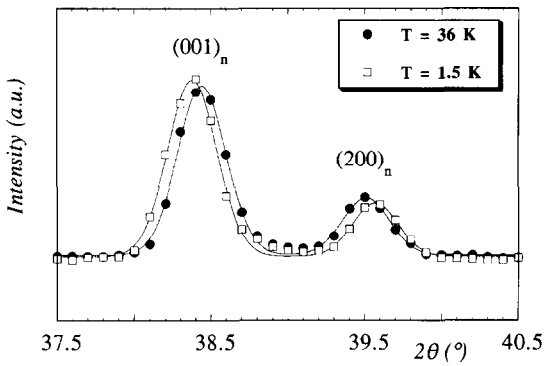

Fig. 6. Part of the neutron powder diffraction pattern of U_2Ni_2Sn ($\lambda = 2.426$ Å) at $T = 36$ and 1.5 K: comparison of the 2θ Bragg angle of the (001) and (200) nuclear peaks.

$U_1 \quad (x \quad \frac{1}{2}+x \quad \frac{1}{4}) \quad M$

$U_2 \quad (-x \quad \frac{1}{2}-x \quad \frac{1}{4}) \quad M$

$U_3 \quad (\frac{1}{2}+x \quad -x \quad \frac{1}{4}) \quad -M$

$U_4 \quad (\frac{1}{2}-x \quad x \quad \frac{1}{4}) \quad -M$

$U'_1 \quad (x \quad \frac{1}{2}+x \quad \frac{3}{4}) \quad -M$

$U'_2 \quad (-x \quad \frac{1}{2}-x \quad \frac{3}{4}) \quad -M$

$U'_3 \quad (\frac{1}{2}+x \quad -x \quad \frac{3}{4}) \quad M$

$U'_4 \quad (\frac{1}{2}-x \quad x \quad \frac{3}{4}) \quad M$

The uranium magnetic moments $\pm \boldsymbol{M}$ are located in the ($\boldsymbol{a}$,$\boldsymbol{b}$) plane of the tetragonal cell. The uranium moment value is $M = 1.05(5)\,\mu_B$ at $T = 1.5$ K.

At $T = 1.5$ K, the lattice parameters are $a = 7.203(3)$ Å and $c = 3.713(2)$ Å. As can be clearly seen in Fig. 6, these parameters show different thermal dependences: from $T = 36$ to 1.5 K, the a-value decreases whereas the c-value increases.

3.3. Mössbauer study

The ^{119}Sn Mössbauer spectrum of U_2Ni_2Sn has been obtained at various temperatures ranging from room temperature to 4.2 K (Fig. 7). At $T = 293$ and 36.5 K, in the paramagnetic region, the spectrum exhibits a quadrupole splitting (QS), as the Sn site possesses a tetragonal point symmetry (Table 4). At 4.2 K, in the antiferromagnetic state, this quadrupole doublet does not show any broadening due to the presence of a magnetic hyperfine field at the Sn site. This result is in agreement with the fact that the magnetic moments of uranium are ordered antiferromagnetically in such a way that the resulting field at the Sn site is zero. The QS at 4.2 K, 0.35(1) mms^{-1}, is comparable to that observed at room temperature.

Table 4
Mössbauer data for U_2Ni_2Sn

T (K)	IS (mms^{-1})	QS (mms^{-1})	Γ (mms^{-1})
293	1.86(1)	0.37(1)	0.81(1)
36.5	1.94(1)	0.36(1)	0.91(1)
4.2	1.93(1)	0.35(1)	0.92(1)

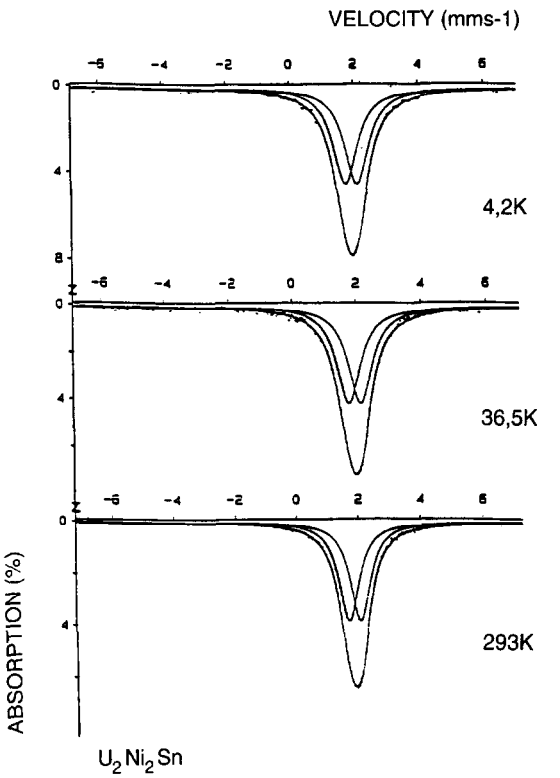

Fig. 7. ^{119}Sn Mössbauer spectrum of U_2Ni_2Sn in the paramagnetic ($T = 293$, 36.5 K) and antiferromagnetic ($T = 4.2$ K) regions. The calculated profile is shown by the full line.

4. Discussion

Neutron powder diffraction experiments performed on two different polycrystalline samples of U_2Ni_2Sn confirm the antiferromagnetic ordering previously observed by magnetic measurements [4,7]. The U_2Ni_2Sn magnetic structure (Fig. 5) is collinear, with:

(1) the uranium magnetic moments ($1.05(5)\mu_B$ at 1.5 K) aligned in the basal plane ($\boldsymbol{a},\boldsymbol{b}$); but no preferential direction with respect to the $\boldsymbol{a}$ and $\boldsymbol{b}$ axis can be deduced from our study,

(2) no ordered magnetic moment at the Ni site.

Since the U_2Ni_2Sn magnetic order is the result of a competition between exchange interactions, crystal field and hybridization effects, we shall consider these effects subsequently.

In the uranium sublattice, each U atom has one U nearest neighbour (NN), located in the ($\boldsymbol{a},\boldsymbol{b}$)-plane at $d_{NN} = 3.575$ Å, two U next-nearest neighbours (NNN) laying in line parallel to the $\boldsymbol{c}$-axis at $d_{NNN} = 3.693$ Å and four next-next nearest neighbours (NNNN) in the basal plane at $d_{NNNN} = 3.799$ Å. So, in a molecular field model, the results of neutron diffraction experiments lead to the following exchange integral scheme: $J_{NN} > 0$, $J_{NNN} < 0$ and $J_{NNNN} < 0$.

Let us now consider the crystal field (CF) effects in U_2Ni_2Sn. In this compound, each uranium atom is surrounded by 6 Ni and 4 Sn ligands arranged in a coordination polyhedron of C_{2v} symmetry (Fig. 2). For such a CF symmetry, when the crystal field is considerably stronger than the other effects (i.e. when the crystal field decides about the direction of the magnetic moment in the ordered state), there is either an easy magnetization axis (C_{2v} axis), or an easy magnetization plane (perpendicular to the C_{2v} axis). However, in the crystallographic unit cell of U_2Ni_2Sn, each of the four uranium atoms has its C_{2v} axis rotated by an angle $\pi/2$ with respect to the other. This would mean that the magnetic moment arrangement within a chemical cell is like any of the models described in Fig. 4, with magnetic moments parallel (or perpendicular) to the [110] (U_1 and U_2) and [1$\bar{1}$0] directions (U_3 and U_4). Since analysis of the neutron powder data excluded all of these arrangements, it seems evident that in U_2Ni_2Sn the hybridization effects are more important than the CF effects (it has already been shown in the literature [14–16] that hybridization effects can seriously reduce CF 'strength').

As for the hybridization effects, let us first consider direct 5f–5f overlapping, since the shortest U–U distance in U_2Ni_2Sn ($d_{NN} = 3.575$ Å) is comparable to the Hill limit [12]. Such a short distance could point out a partial delocalization of the 5f electrons. However, the relevant U–U pairs (Fig. 2) do not propagate within the crystal structure, either as chains or as layers, so that the single pair 5f–5f overlap, having no translational periodicity, will not lead to a strong itinerancy.

More serious delocalization of the 5f electrons may arise from the hybridization with the ligand electrons. As seen from Fig. 2 and Table 2, uranium in U_2Ni_2Sn is surrounded by two Ni atoms at 2.772 Å, 4 Ni atoms at 2.873 Å (and further four Sn atoms at 3.260 Å). Considering the U–Ni interatomic distances only is not sufficient for an accurate evaluation of the hybridization effects, as will be illustrated in the following examples: U_2Ni_2Sn, UNiSn and UNi_2Sn. These U_xNi_ySn ternary compounds have similar U–Ni distances (UNi_2Sn [17,18] shows a structural transition, from cubic to orthorhombic, around 220 K; at this transition, the average U–Ni distance increases (2.868 Å at 80 K, shortest U–Ni distance = 2.672 Å) and the magnetic susceptibility (orthorhombic phase) is enhanced). While U_2Ni_2Sn and UNiSn [19] are antiferromagnetically ordered at low temperature, UNi_2Sn is not magnetically ordered [17]. More important for the hybridization effects seems to be in this case the number of nearest Ni ligands which amount to 4, 6 and 8 for UNiSn, U_2Ni_2Sn and UNi_2Sn, respectively. In this way one may expect that the hybridization effects for U_2Ni_2Sn with $T_N = 25$ K and $M = 1.05\mu_B$ are stronger than those for UNiSn, which orders antiferromagnetically at $T_N = 45$ K with $M = 1.4\mu_B$.

Acknowledgements

One of us (TVH) would like to thank LLB and the European Community for financial support during his stay at Saclay. CNRS financial support for ZZ is also gratefully acknowledged.

References

[1] V. Sechovsky and L. Havela, in: Ferromagnetic Materials, eds. E.P. Wohlfarth and K.H.J. Buschow (North-Holland, Amsterdam, 1988), Vol. 4, p. 309.

[2] F. Mirambet, P. Gravereau, B. Chevalier, L. Trut and J. Etourneau, J. Alloys and Compounds 191 (1993) L1.

[3] W.H. Zachariasen, Acta Crystallogr. 2 (1949) 94.

[4] Z. Zolnierek and A. Zaleski, 23èmes Journées des Actinides, 1993, Abstract O6.6.

[5] L. Havela, V. Sechovsky, H. Nakotte, P. Prokes, F.R. de Boer, J.C. Spirlet, Y. Kergadallan and A. Seret, 23èmes Journées des Actinides, 1993, Abstract P1.9.

[6] J.M. Winand, Y. Kergadallan, M.N. Peron, D. Meyer, J. Rebizant and J.C. Spirlet, 23èmes Journées des Actinides, 1993, Abstract P1.10.
[7] F. Mirambet, B. Chevalier, L. Fournès, P. Gravereau and J. Etourneau, J. Alloys and Compounds 203 (1994) 29.
[8] M.N. Peron, Y. Kergadallan, J. Rebizant, D. Meyer, J.M. Winand, S. Zwirner, L. Havela, H. Nakotte, J.C. Spirlet, G.M. Kalvius, E. Colineau, J.L. Oddou, C. Jeandey and J.P. Sanchez, J. Alloys and Compounds 201 (1993) 203.
[9] J. Rodriguez-Carvajal, Powder Diffraction, Satellite Meeting of the XV Congress of IUCr, Toulouse, 1990, Abstract p. 127.
[10] V.F. Sears, Neutron News 3(3) (1992) 26.
[11] P.J. Brown, International Tables for Crystallography, ed. A.J.C. Wilson (Kluwer Academic Publishers, Dordrecht, 1970), Vol. C(4.4.4).
[12] H.H. Hill, Plutonium 1970 and other Actinides, ed. W.N. Miner (AIME, New York, 1970), p. 2.
[13] O.V. Kovalev, Irreducible Representations of the Space Groups (Gordon and Breach, New York, 1955).
[14] K. Takegahara, H. Takahashi, A. Yanase and T. Kasuya, J. Phys. C 14 (1981) 737.
[15] J.M. Wills and B.R. Cooper, Phys. Rev. B 36 (1987) 3809.
[16] P.M. Levy and S. Zhang, Phys. Rev. Lett. 62 (1989) 78.
[17] T. Endstra, S.A.M. Mentink, G.J. Nieuwenhuys, J.A. Mydosh and K.H.J. Buschow, J. Phys.: Condens. Matter 2 (1990) 2447.
[18] A. Drost, W.G. Haije, E. Frikke, T. Endstra, G.J. Nieuwenhuys and K.H.J. Buschow, Solid State Comm. 88 (1993) 327.
[19] M. Yethiraj, R.A. Robinson, J.J. Rhyne, J.A. Gotaas and K.H.J. Buschow, J. Magn. Magn. Mater. 9 (1989) 355.